Integration of a geodetic grade GNSS receiver and an Android dual-frequency smartphone with low-cost IMU for seismogeodetic applications

Caneren GÜL, Taylan ÖCALAN, Erdem DAMCI, Çağla ŞEKERCİ, Türkiye

Keywords: seismogeodesy, Xiaomi Mi8, low-cost MEMS IMU, GNSS / accelerometer integration

SUMMARY

Global Navigation Satellite Systems (GNSS) can effectively provide semi-static and dynamic displacements by kinematic data processing of high rate observables without any numerical integration process unlike classical seismological sensors such as accelerometers. However, the noise amplitude of the high rate GNSS (HR-GNSS) derived displacements is larger than accelerometers due to various error sources mainly originating from residual atmospheric propagation effects and multipath caused by the receiver set-up environment. Recent advances showed that the integration of geodetic grade HR-GNSS displacements with high-quality accelerometers can provide accurate motion tracking for seismogeodetic applications. However, geodetic grade HR-GNSS and high-quality accelerometers are expensive tools together, and seismogeodesy with these high-grade sensors is not cost-effective. In addition to this, in order to perform HR-GNSS/accelerometer loosely-coupled integration, coordinate frames of these sensors must be aligned. In this study, a low-cost Inertial Measurement Unit (IMU) in the Xiaomi Mi8 smartphone was used in the integration of geodetic grade Trimble NetR9 Precise Point Positioning (PPP) HR-GNSS displacements through a Multi-rate Kalman Filter. The 1999 Düzce Earthquake (M_w = 7.2) in Türkiye and the 1989 Loma-Prieta Earthquake (M_w = 6.9) in the United States of America were simulated on a single axis shake table. In order to provide a cost-effective static alignment for the transformation of the smartphone IMU coordinate frame into the local North East Down frame, Singular Value Decomposition (SVD) was used as combining the smartphone accelerometer and the magnetometer sensors. In addition to this, the same procedure was applied for Xiaomi Mi8 dual-frequency GNSS displacements and accelerometer integration. The Root Mean Square (RMS) values of Trimble NetR9 GNSS/smartphone accelerometer for the Düzce and the Loma-Prieta Earthquake experiments are 4.7 mm and 5.4 mm, respectively. The RMS values of Xiaomi Mi8 dual-frequency GNSS/accelerometer integration are 279 mm for the Düzce Earthquake and 96.7 mm for the Loma-Prieta Earthquake experiments. Results indicate that the integration of geodetic grade HR-GNSS with low-cost IMU is suitable for seismogeodetic applications, whereas Xiaomi Mi8 GNSS/accelerometer integration produces large-scale errors due to the high uncertainty of its dual-frequency GNSS solutions.

Integration of a geodetic grade GNSS receiver and an Android dual-frequency smartphone with low-cost IMU for seismogeodetic applications

Caneren GÜL, Taylan ÖCALAN, Erdem DAMCI, Çağla ŞEKERCİ, Türkiye

1. INTRODUCTION

Nowadays, Global Navigation Satellite Systems (GNSS) have become a classical way to obtain coseismic displacements as an alternative to double integration of seismic grade accelerometer sensors. High-rate GNSS (HR-GNSS) enables to yield dynamic displacements for seismologic studies. This ability led to form the concept of seismogeodesy (Larson et al., 2003; Bock et al., 2004; Larson, 2009).

With the Precise Point Positioning (PPP) (Zumberge et al., 1997), precise positioning has become possible with stand-alone GNSS receivers. In Kouba (2003), 1 Hz sampled Global Positioning System (GPS) data from reference stations processed using kinematic PPP for investigating the displacement accuracy of the 2002 Denali Fault Earthquake (M_w = 7.9), Alaska, and the 2003 Honshi Earthquake (M_w = 7.0), Japan. This study showed that displacements derived from kinematic PPP confirm the displacements obtained earlier by Larson (2003) for the Denali Fault Earthquake. In Ohta et al. (2008), estimated coseismic displacements with kinematic PPP agreed with displacements derived from collocated accelerometers. Colosimo et al. (2011) proposed a method for the estimation of real-time displacements using stand-alone GNSS receivers based on epoch differencing of high-rate carrier phase GNSS measurements. Xu et al. (2013) showed that 50 Hz PPP is capable of detecting horizontal and vertical displacements at mm and subcentimeter levels, respectively.

Thanks to the complementarity of GNSS and seismic sensors, broadband coseismic displacements can be accurately captured by their integration (Bock et al., 2011; Geng et al., 2013; Tu et al., 2017). GNSS-derived displacements and the dynamic inputs that are measured by seismic sensors can be integrated with a Kalman Filter framework. Smyth and Wu (2007) proposed a Multi-rate Kalman Filter in which the sampling frequency of seismic sensors is integer multiple of the sampling frequency of GNSS displacements. Therefore the dynamic estimates of parameters are updated when the measurements are available at regular timestamps. Bock et al. (2011) used Multi-rate Kalman Filter for real-time monitoring tests on the 2010 El Mayor-Cucapah Earthquake (M_w = 7.2). Saunders et al. (2016) efficiently integrated GPS displacements with a relatively low-cost micro-electro-mechanical sensor (MEMS) accelerometer that has developed at Scripps Institution of Oceanography (SIO). Recently, Xin et al. (2021) introduced Strong Motion Accelerographs with GNSS 2000 (SMAG2000), allowing the real-time estimation of displacements with loosely coupled and tightly coupled multi-rate Kalman Filter + near-real-time smoother.

The combination of geodetic grade GNSS and seismic grade accelerometer results in high costs for seismogeodetic applications. In this study, 5 Hz Trimble NetR9 geodetic grade GNSS receiver PPP displacements and a low-cost 100 Hz InvenSense ICM20690 IMU in Xiaomi Mi8 smartphone are integrated through the multi-rate Kalman Filter for coseismic displacement estimation. The 1999 Düzce Earthquake (M_w = 7.2) in Turkey and the 1989 Loma-Prieta Earthquake (M_w = 6.9) in the United States of America were simulated on a single-axis shake table. We utilized the Singular Value Decomposition (SVD) method (Markley, 1988) and employed stationary smartphone IMU accelerometer readings together with magnetometer sensor outputs to perform static alignment of GNSS displacements and accelerations into the local North East Down tangent coordinate frame. After the alignment step, displacements were estimated using the multi-rate Kalman Filter. The same procedures were applied for 1 Hz Xiaomi Mi8 dual-frequency PPP GNSS and smartphone IMU integration. In section 2, the multi-rate Kalman Filter scheme and static alignment with SVD are explained. The results of Trimble NetR9 PPP GNSS/accelerometer integration and Xiaomi Mi8 dual-frequency PPP GNSS/accelerometer integration are presented in section 3.

2. METHODOLOGY

2.1 Multi-rate Kalman Filter

Kalman Filter is a state estimation method that optimally combines measurements with the dynamics of state parameters. In a discrete-time Kalman Filter, the dynamic update equation is given as (Catlin, 1989):

$$\boldsymbol{x}_{\boldsymbol{k+1}}^{-} = \boldsymbol{\Phi}_{\boldsymbol{k}}\boldsymbol{x}_{\boldsymbol{k}}^{+} + \boldsymbol{B}_{\boldsymbol{k}}\boldsymbol{u}_{\boldsymbol{k}} + \boldsymbol{w}_{\boldsymbol{k}}$$

$$\boldsymbol{P}_{\boldsymbol{k+1}}^{-} = \boldsymbol{\Phi}\boldsymbol{P}_{\boldsymbol{k}}^{+}\boldsymbol{\Phi}^{\boldsymbol{T}} + \boldsymbol{Q}$$

where $\boldsymbol{x}^{-}$ is the dynamic estimate of the state vector, $\boldsymbol{x}^{+}$ is the filtered state vector, $\boldsymbol{\Phi}$ is the state transition matrix, $\boldsymbol{u}$ is the dynamic input, $\boldsymbol{B}$ is the input matrix and $\boldsymbol{w}$ is the vector of discrete-time dynamic noise process. The dynamic estimate variance-covariance is indicated as $\boldsymbol{P}^{-}$ and $\boldsymbol{Q}$ is the variance-covariance matrix of the dynamic noise process w. Dynamic estimate is filtered when the measurements are available.

$$\boldsymbol{y}_{\boldsymbol{k+1}} = \boldsymbol{H}\boldsymbol{x}_{\boldsymbol{k+1}}^{+} + \boldsymbol{\alpha}_{\boldsymbol{k+1}}$$

$$\boldsymbol{x}_{\boldsymbol{k+1}}^{+} = \boldsymbol{x}_{\boldsymbol{k+1}}^{-} + \boldsymbol{K}_{\boldsymbol{k+1}}(\boldsymbol{y}_{\boldsymbol{k+1}} - \boldsymbol{H}\boldsymbol{x}_{\boldsymbol{k+1}}^{-})$$

$$\boldsymbol{P}_{\boldsymbol{k+1}}^{+} = (\boldsymbol{1} - \boldsymbol{K}_{\boldsymbol{k+1}}\boldsymbol{H})\boldsymbol{P}_{\boldsymbol{k+1}}^{-}$$

The observation vector $\boldsymbol{y}$ is the function of the filtered state vector and $\boldsymbol{\alpha}$ is the observation noise that is assumed uncorrelated with dynamic process noise $\boldsymbol{w}$. The term $\boldsymbol{K}$ is the Kalman

gain that corrects dynamic estimate of state vector. $\boldsymbol{P}^{+}$ is the variance-covariance matrix of the filtered state vector.

When the sampling rate of observations and accelerations are different, measurement updates cannot be performed at every timestamp. Dynamic updates of state parameters are performed until the next observation is available. Smyth and Wu (2007) proposed a Multi-rate Kalman Filter for the case of different sampling rates of sensors. The ratio of the sampling period of the accelerometer sensor and displacement measurement is,

$$M = \frac{\Delta t_d}{\Delta t_a}$$

where Δt_d is the sampling period of displacement measurements, Δt_a is the sampling period of acceleration readings and M is the integer. In GNSS/accelerometer integration schemes, the sampling rate of the accelerometer sensor is usually greater than the sampling rate of GNSS displacements. When M is set as an integer, measurement updates can be performed at regular intervals. The discrete-time dynamic update equations for displacements can be expressed as (Smyth & Wu, 2007; Bock et al., 2011) below,

$$\begin{bmatrix} d_{k+1}^{-} \\ v_{k+1}^{-} \end{bmatrix} = \begin{bmatrix} 1 & \Delta t_a \\ 0 & 1 \end{bmatrix} \begin{bmatrix} d_k^{+} \\ v_k^{+} \end{bmatrix} + \begin{bmatrix} \Delta t_a^2 \\ \Delta t_a \end{bmatrix} u_k + w_k$$

where d and v are displacements and velocity parameters, respectively. w is the equivalent discrete-time noise process of uncorrelated white noise with variance q. The discrete-time covariance matrix of dynamic noise process w_k at time k is given by:

$$\boldsymbol{Q} = \begin{bmatrix} \frac{q\Delta t_a^3}{3} & \frac{q\Delta t_a^2}{2} \\ \frac{q\Delta t_a^2}{2} & q\Delta t_a \end{bmatrix}$$

2.2 Static Alignment with Singular Value Decomposition

Conversion of GNSS displacements in earth-centered and earth-fixed (ECEF) frame to the north east down local tangent frame (NED frame) is a well-known procedure in geodetic literature. The transformation from ECEF coordinates to NED coordinates can be given by (Jekeli, 2012):

$$\begin{bmatrix} n \\ e \\ d \end{bmatrix} = \begin{bmatrix} -sin\varphi cos\lambda & -sin\varphi cos\lambda & cos\lambda \\ -sin\lambda & cos\lambda & 0 \\ -cos\lambda cos\varphi & -cos\varphi sin\lambda & -sin\varphi \end{bmatrix} \begin{bmatrix} X - X_0 \\ Y - Y_0 \\ Z - Z_0 \end{bmatrix}$$

Here, X, Y, Z are ECEF coordinates and X_0, Y_0, Z_0 are reference coordinates for NED frame conversion.

In order to perform the integration of GNSS displacements with IMU, the orientation of IMU sensor frame with respect to NED frame is required. A static alignment algorithm based on Singular Value Decomposition (SVD), proposed by Markley (1988) can be used to determine IMU sensor frame orientation with respect to the NED frame. Thus, accelerometer sensor readings can be converted to NED frame and GNSS/accelerometer integration can be done successfully.

The static alignment algorithm tries to minimize a least-squares cost function (Shuster & Oh, 1981):

$$L(\boldsymbol{A}) = 0.5 \sum_{i=1}^{n} a_i |b_i - \boldsymbol{A} r_i|^2$$

$$L(\boldsymbol{A}) = \lambda_0 - \sum_{i=1}^{n} a_i b_i^T \boldsymbol{A} r_i = \lambda_0 - tr(\boldsymbol{A}\boldsymbol{B}^{\boldsymbol{T}})$$

$$\boldsymbol{B} = \sum_{i=1}^{n} a_i b_i {r_i}^T$$

$\boldsymbol{A}$ is the transformation matrix that minimizes the cost function $L(\boldsymbol{A})$. $\boldsymbol{b}$ is the vector of sensor readings in the sensor frame and $\boldsymbol{r}$ is the vector of sensor outputs in the target frame. The term λ_0 is the normalized weights of sensors.

SVD method applies singular value decomposition on matrix **B** (Markley, 1988):

$$\boldsymbol{B} = \boldsymbol{U}\boldsymbol{S}\boldsymbol{V}^{\boldsymbol{T}}$$

The orthogonal matrices U and V are replaced with proper orthogonal matrices to guarantee their determinants are equal to 1 and the matrix **A** is reconstructed with these new orthogonal matrices (Markley, 1988):

$$\boldsymbol{U}^{+} = \boldsymbol{U}[diag(1,1,det\boldsymbol{U})]$$

$$\boldsymbol{V}^{+} = \boldsymbol{V}[diag(1,1,det\boldsymbol{V})]$$

$$\mathbf{A} = \boldsymbol{U}^{+}\boldsymbol{V}^{+\boldsymbol{T}}$$

Proper orthogonal matrices are useful particularly when the matrix **B** is singular. In order to apply SVD method, two or more sensors are required (Markley, 1988; Hajiyev et al., 2015).

Stationary accelerometer sensor readings can provide the information for roll and pitch angles with respect to NED frame. For yaw angle, magnetometer sensors can be added (Groves, 2013). Target frame vectors for magnetometer sensors can be obtained from World Magnetic Model (URL-1) or International Geomagnetic Reference Frame (Alken et al., 2021; URL-2).

3. RESULTS

In Multi-rate Kalman Filter, 5 Hz Trimble NetR9 PPP GNSS displacements were used as measurement process and 100 Hz accelerometer readings of InvenSense ICM20690 IMU in Xiaomi Mi8 were used as dynamic input. Collected GNSS data were processed with RTKLiB open-source GNSS data processing software (Takasu, 2013). GNSS data processing strategy is summarized in Table 1:

Parameters	Solution / Product Used
Precise Ephemerides	CNES*
Precise Clock	CNES
*TEC**	CODE*
Zenith Wet Delay	Zenith Total Delay Estimated
Ambiguity Resolution	Float

** CNES: Centre national d'études spatiales, CODE: Center for Orbit Determination in Europe, TEC: Total Electron Content*

Table 1: GNSS data processing strategy in RTKLiB

ECEF WGS84 PPP GNSS displacements were transformed into NED frame. In order to align accelerometer sensor readings to NED frame, ak0991 magnetometer sensor in Xiaomi Mi8 combined with accelerometer using SVD method as introduced in section 2.

To test Multi-rate Kalman Filter with SVD method, scaled displacement waveforms (by a factor of 1/15) of the 1999 Düzce Earthquake and 1989 Loma-Prieta Earthquake were simulated using the SARSAR single-axis shake table (Damcı & Şekerci, 2019). In case of data loss or internal failure of Trimble NetR9 receiver, another geodetic grade receiver Topcon Hiper-SR was mounted on the shake table.

We first analyzed the displacement estimation results of 5 Hz Trimble NetR9 PPP GNSS/100 Hz accelerometer Multi-rate Kalman Filter integration. Results of the 1999 Düzce Earthquake are illustrated in Figure 1. It can be seen from Figure 1 that the results of the Multi-rate Kalman Filter are close to shake table records of the earthquake. The displacement RMS value of the 1999 Düzce Earthquake is 4.7 mm.

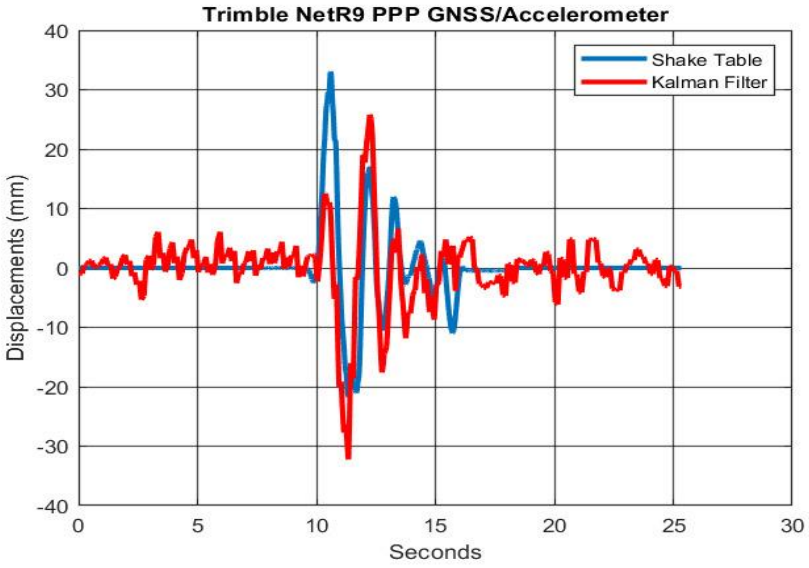

Figure 1: Estimated displacement waveforms of the 1999 Düzce Earthquake, Turkey (M_w = 7.2) with 5 Hz Trimble NetR9 PPP GNSS/100 Hz Mi8 accelerometer integration.

Displacement estimation results for the 1989 Loma-Prieta Earthquake is illustrated in Figure 2. As in the 1999 Düzce Earthquake experiment, outputs of the Multi-rate Kalman Filter are parallel to the shake table displacement records. The displacement RMS value of the 1989 Loma-Prieta Earthquake is 5.4 mm.

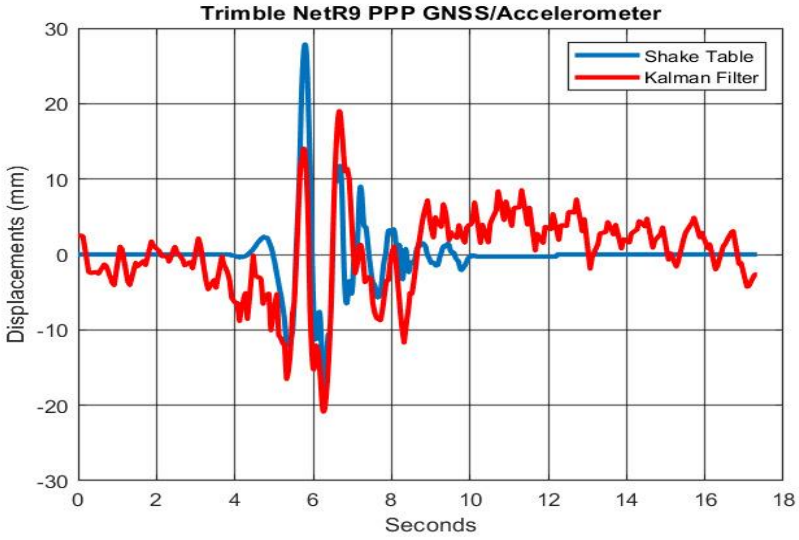

Figure 2: Estimated displacement waveforms of the 1989 Loma-Prieta Earthquake (M_w = 6.9) with 5 Hz Trimble NetR9 PPP GNSS/100 Hz Mi8 accelerometer integration.

In Xiaomi Mi8 dual-frequency 1 Hz PPP GNSS/100 Hz accelerometer integration, GNSS displacements shows dm level deviations, where the range of displacements of the earthquakes are cm. In Figure 3, displacement estimation results of the 1999 Düzce Earthquake were illustrated. The displacement RMS value is 279 mm.

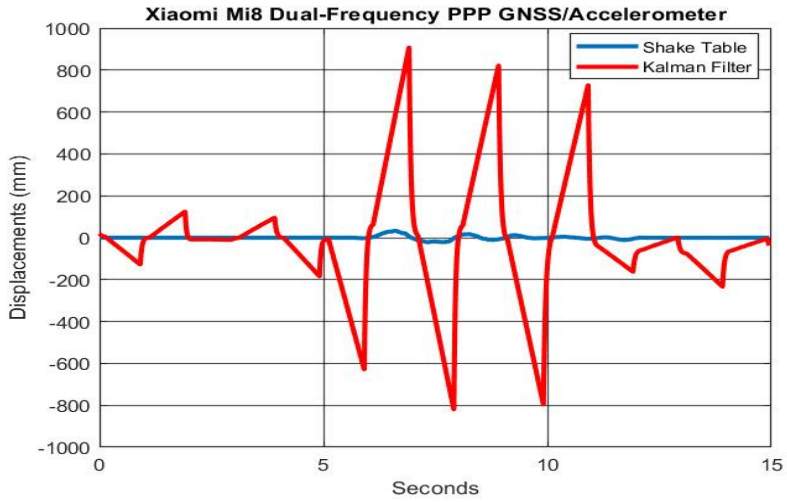

Figure 3: Estimated displacement waveforms of the 1999 Düzce Earthquake, Turkey (M_w = 7.2) with 1 Hz Xiaomi Mi8 dual-frequency PPP GNSS/100 Hz accelerometer integration.

Results of the 1989 Loma-Prieta Earthquake are illustrated in Figure 4. Displacement estimations show large-scale deviations. The calculated displacement RMS value is 96.7 mm.

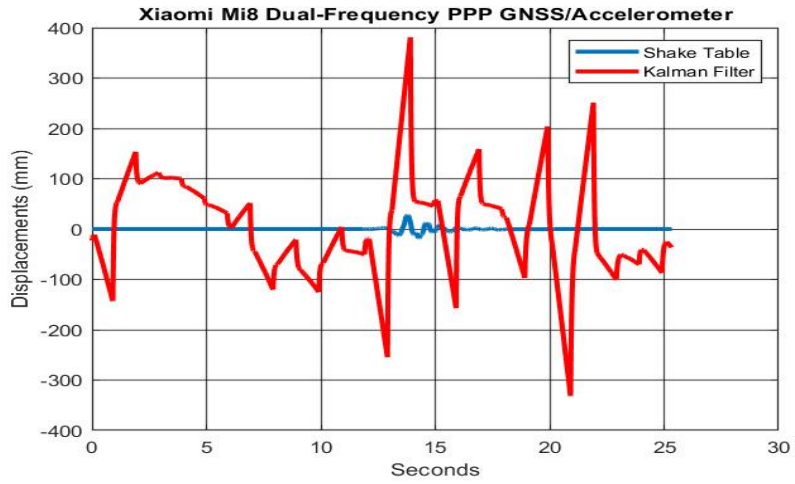

Figure 4: Estimated displacement waveforms of the 1989 Loma-Prieta Earthquake (M_w = 6.9) with 1 Hz Xiaomi Mi8 dual-frequency PPP GNSS/100 Hz accelerometer integration.

All results show that the quality of Multi-rate Kalman Filter outputs is highly dependent on the quality of displacement measurements. The sampling rate of Trimble NetR9 PPP GNSS displacements was 5 Hz and Xiaomi Mi8 dual-frequency PPP GNSS was 1 Hz. This indicates that the multi-rate factors M for Trimble NetR9 and Xiaomi Mi8 are 20 and 1, respectively. The 5 Hz sampling rate efficiently captures the displacement waveform. Xiaomi Mi8 has a lower sampling rate than geodetic grade GNSS and collected observables are of poor quality. Geodetic-grade GNSS receivers can be integrated with low-cost accelerometers for seismogeodetic applications. On the other hand, Xiaomi Mi8 dual-frequency GNSS is not suitable enough for seismogeodetic applications and its accuracy needs to be improved.

ACKNOWLEDGEMENTS

Authors would like to thank Tomoji Takasu for RTKLiB open-source GNSS data processing software, Istanbul University Cerrahpasa Structure & Mechanics Laboratory for technical support for experiments. Authors also thank to the Centre national d'études spatiales (CNES) and the Center for Orbit Determination in Europe (CODE) for multi-GNSS precise products.

REFERENCES

Alken, P., Thébault, E., Beggan, C. D., Amit, H., Aubert, J., Baerenzung, J., ... & Zhou, B. (2021). International geomagnetic reference field: the thirteenth generation. *Earth, Planets and Space*, *73*(1), 1-25.

Bock, Y., Prawirodirdjo, L., & Melbourne, T. I. (2004). Detection of arbitrarily large dynamic ground motions with a dense high-rate GPS network. *Geophysical Research Letters*, *31*(6).

Bock, Y., Melgar, D., & Crowell, B. W. (2011). Real-time strong-motion broadband displacements from collocated GPS and accelerometers. *Bulletin of the Seismological Society of America*, *101*(6), 2904-2925.

Catlin, D. E. (1989). *Estimation, control, and the discrete Kalman filter*. Springer.

Colosimo, G., Crespi, M., & Mazzoni, A. (2011). Real-time GPS seismology with a stand-alone receiver: A preliminary feasibility demonstration. *Journal of Geophysical Research: Solid Earth*, *116*(B11).

Damcı, E., & Şekerci, Ç. (2019). Development of a low-cost single-axis shake table based on arduino. *Experimental Techniques*, *43*(2), 179-198.

Geng, J., Bock, Y., Melgar, D., Crowell, B. W., & Haase, J. S. (2013). A new seismogeodetic approach applied to GPS and accelerometer observations of the 2012 Brawley seismic swarm: Implications for earthquake early warning. *Geochemistry, Geophysics, Geosystems*, *14*(7), 2124-2142.

Groves, P. (2013). *Principles of GNSS, Inertial, and Multisensor Integrated Navigation Systems, Second Edition*. Artech House.

Hajiyev, C., Çilden, D., & Somov, Y. (2015). Gyroless attitude and rate estimation of small satellites using singular value decomposition and extended Kalman filter. In *Proceedings of the 2015 16th International Carpathian Control Conference (ICCC)* (pp. 159-164). IEEE.

Jekeli, C. (2012). *Inertial navigation systems with geodetic applications*. de Gruyter.

Kouba, J. (2003). Measuring seismic waves induced by large earthquakes with GPS. *Studia Geophysica et Geodaetica*, *47*(4), 741-755.

Larson, K. M., Bodin, P., & Gomberg, J. (2003). Using 1-Hz GPS data to measure deformations caused by the Denali fault earthquake. *Science*, *300*(5624), 1421-1424.

Larson, K. M. (2009). GPS seismology. *Journal of Geodesy*, *83*(3), 227-233.

Markley, F.L. (1988). Attitude determination using vector observations and the singular value decomposition. *Journal of The Astronautical Sciences*, *36*, 245-258.

Ohta, Y., Ohzono, M., Miura, S., Iinuma, T., Tachibana, K., Takatsuka, K., ... & Umino, N. (2008). Coseismic fault model of the 2008 Iwate-Miyagi Nairiku earthquake deduced by a dense GPS network. *Earth, planets and space*, *60*(12), 1197-1201.

Saunders, J. K., Goldberg, D. E., Haase, J. S., Bock, Y., Offield, D. G., Melgar, D., ... & Mattioli, G. S. (2016). Seismogeodesy using GPS and low-cost MEMS accelerometers: Perspectives for earthquake early warning and rapid response. *Bulletin of the Seismological Society of America*, *106*(6), 2469-2489.

Shuster, M. D., & Oh, S. D. (1981). Three-axis attitude determination from vector observations. *Journal of guidance and Control*, *4*(1), 70-77.

Smyth, A., & Wu, M. (2007). Multi-rate Kalman filtering for the data fusion of displacement and acceleration response measurements in dynamic system monitoring. *Mechanical Systems and Signal Processing*, *21*(2), 706-723.

Takasu, T. (2013). RTKLIB ver. 2.4. 2 Manual. *RTKLIB: An Open Source Program Package for GNSS Positioning*, 29-49.

Tu, R., Liu, J., Lu, C., Zhang, R., Zhang, P., & Lu, X. (2017). Cooperating the BDS, GPS, GLONASS and strong-motion observations for real-time deformation monitoring. *Geophysical Journal International*, *209*(3), 1408-1417.

URL1: https://www.ngdc.noaa.gov/geomag/WMM/ (Date of access: February 1, 2022)

URL2: https://www.ngdc.noaa.gov/IAGA/vmod/igrf.html (Date of access: February 1, 2022)

Xin, S., Geng, J., Zeng, R., Zhang, Q., Ortega-Culaciati, F., & Wang, T. (2021). In-situ real-time seismogeodesy by integrating multi-GNSS and accelerometers. *Measurement*, *179*, 109453.

Xu, P., Shi, C., Fang, R., Liu, J., Niu, X., Zhang, Q., & Yanagidani, T. (2013). High-rate precise point positioning (PPP) to measure seismic wave motions: an experimental comparison of GPS PPP with inertial measurement units. *Journal of Geodesy*, *87*(4), 361-372.

Zumberge, J. F., Heflin, M. B., Jefferson, D. C., Watkins, M. M., & Webb, F. H. (1997). Precise point positioning for the efficient and robust analysis of GPS data from large networks. *Journal of geophysical research: solid earth*, *102*(B3), 5005-5017.

BIOGRAPHICAL NOTES

Research Assis. Caneren GÜL, B.Sc.
Caneren GÜL completed his undergraduate education in 2018 at Yildiz Technical University Department of Geomatic Engineering. He is a MSc. student at Yildiz Technical University Geomatic Engineering Program since 2019. His research interests are stochastic processes and applied optimal estimation.

Associate Prof. Taylan Öcalan, Ph.D.
Taylan Öcalan graduated in 2005 with a degree of M.Sc. at the Graduate School of Science and Engineering of Yildiz Technical University and the topic of his thesis was the investigation of relative point positioning accuracy based on permanent GPS stations. He received his Ph.D. degree in 2015 about GNSS Precise Point Positioning. His research interests include high-accurate Global Navigation Satellite Systems applications, smart device sensor integration for positioning, PPP, hydrographical surveys and engineering surveys. He currently works as associate professor in Yildiz Technical University since 2019.

Assistant Prof. Erdem DAMCI, Ph.D.

Erdem DAMCI completed his undergraduate, graduate, and doctorate degrees at Istanbul University, Department of Civil Engineering. He started to work as an Assistant Professor at Istanbul University, Faculty of Engineering, Department of Civil Engineering, in 2011 and continues this duty at Istanbul University-Cerrahpasa, Faculty of Engineering, Department of Civil Engineering. In addition to his theoretical studies, he also conducts experimental research, and his subjects of study include the design and implementation of low-cost laboratory equipment, shake table experiments, ambient vibration analysis, and image processing techniques.

Research Assis. Çağla ŞEKERCİ, M.Sc.

Çağla ŞEKERCİ completed her undergraduate education in 2014 and her master's degree in 2018 at Istanbul University, Department of Civil Engineering. She continues her Ph.D. studies, which she started in 2018, at Istanbul University-Cerrahpasa, Department of Civil Engineering, and she has been working as a Research Assistant at Doğuş University Department of Civil Engineering since 2017. Her research interests include the design and implementation of low-cost laboratory equipment, shake table experiments, ambient vibration analysis, and image processing techniques.

CONTACTS

Research Assis. Caneren GÜL, B.Sc.
Yildiz Technical University
Faculty of Civil Engineering, Department of Geomatic Engineering, Davutpasa Campus, Esenler/Istanbul
Türkiye
Tel. +90 212 383 53 33
Email: cgul@yildiz.edu.tr
Web site: https://avesis.yildiz.edu.tr/cgul

Associate Prof. Taylan ÖCALAN, Ph.D.
Yildiz Technical University
Faculty of Civil Engineering, Department of Geomatic Engineering, Davutpasa Campus, Esenler/Istanbul
Türkiye
Tel. +90 212 383 53 02
Email: tocalan@yildiz.edu.tr
Web site: http://avesis.yildiz.edu.tr/tocalan

Assistant Prof. Erdem DAMCI, Ph.D.
Istanbul University Cerrahpasa
Faculty of Engineering, Department of Civil Engineering, Avcilar Campus, Avcilar
Istanbul
Faculty of Engineering, Department of Civil Engineering, Structure & Mechanics Laboratory
Buyukcekmece Campus, Buyukcekmece
Istanbul
Türkiye
Tel. +90 212 473 70 70
Email: edamci@iuc.edu.tr
Web site: http://www.erdemdamci.com

Research Assis. Çağla ŞEKERCİ, M.Sc.
Dogus University
Faculty of Engineering, Department of Civil Engineering, Dudullu Campus, Umraniye
Istanbul
Istanbul University Cerrahpasa
Faculty of Engineering, Department of Civil Engineering, Structure & Mechanics Laboratory
Buyukcekmece Campus, Buyukcekmece
Istanbul
Türkiye
Tel. +90 212 473 70 70
Email: csekerci@dogus.edu.tr